Journal of Inclusion Phenomena and Molecular Recognition in Chemistry **24:** 241–262, 1996.

Crystal Inclusion Chemistry of Zinc-Tetra(4-Bromophenyl)Porphyrin

PARTHASARATHI DASTIDAR, HELENA KRUPITSKY, ZAFRA STEIN and ISRAEL GOLDBERG*
School of Chemistry, Sackler Faculty of Exact Sciences, Tel Aviv University, 69978 Ramat Aviv, Tel Aviv, Israel.

Received: 7 November 1995; In final form: 26 January 1996

Abstract. The structural patterns of Zn(II)-tetra(4-bromophenyl)porphyrin and several of its newly prepared complexes and clathrates in the solid phase were determined by X-ray crystallography. The molecular structure of the porphyrin compound is characterized by a nearly perfect planarity of the metalloporphyrin core due to effective Zn···Br intermolecular interactions in the crystalline lattice. The composite materials show three different kinds of interporphyrin organization, dominated to a large extent by the molecular shape, often exhibited by related tetraphenylporphyrin derivatives. These include monoclinic 'herringbone' packing modes without any apparent involvement of the halogen atoms in specific interactions, chained interporphyrin arrangements exhibiting C—Br···π close approach, and porous layered networks of the porphyrin species revealing direct Br···Br contacts. The latter two forms are also affected by C—H···Br attractions. Four-, five- and six-coordination of the central zinc ion was observed, but there is no apparent correlation between the coordination number and the crystal packing type. Thermal analysis revealed the relative strength of binding of the ligand and solvate species to the porphyrin lattice. The bromophenyl-substituted porphyrin building block forms only a small number of crystalline heteromolecular materials with other components, and occurrence of the uniquely structured porous porphyrin networks is not as dominant as in the analogous chlorophenyl derivatives. Estimates of interporphyrin packing stabilization energies suggest that the stability of these layered patterns is affected primarily by dipolar attractions, which are less significant in solids containing the Br, rather than Cl, groups.

Key words. Zinc-tetra(4-bromophenyl)porphyrin, crystal inclusion chemistry of, coordination features of Zn(II), weak interactions involving halogen atoms.

Supplementary Data relating to this article have been deposited with the British Library as supplementary publication No. SUP 82200 (40 pages).

1. Introduction

The versatility of the tetraarylporphyrin compounds as crystalline hosts appears to be unequaled due to the large size, high symmetry, rigidity, and thermal stability of the molecular framework. It is also feasible to tailor their shape and functionality features by organic synthesis, and thus affect the microstructure of the resulting assembly. Crystalline aggregation of unsubstituted tetraphenylmetalloporphyrins was found to be dominated primarily by the molecular shape and

* Author for correspondence.

dispersion forces. It yields, in most cases, hollow interporphyrin architectures, which provide the driving force for the incorporation of a 'guest' component into the crystal lattice [1–4]. A suitable functionalization of the rigid metalloporphyrin molecular framework with polarized aryl groups by deliberate synthesis can be used to affect in a pre-programmed way the spontaneous build-up of the porphyrin lattice by molecular recognition properties of the respective sensor groups. The resulting nanostructures have a hollow, cross-linked, pseudo-rigid supramolecular architecture, and provide novel types of potential solid state receptors for isolation, separation, transport, exchange and controlled release of molecular entities. Our earlier preparative efforts have yielded several new classes of crystalline polymer-type aggregates, in which the functionalized porphyrin host units are rigidly linked, through hydrogen bonds or metal-to-ligand coordination, into multi-dimensional porous polymeric patterns [5, 6]. Motifs of crystalline intermolecular organization in porphyrins tetra-substituted by 4-chlorophenyl and 4-fluorophenyl groups, and the inclusion properties of these materials, have also been recently characterized [6, 7]. In many of the chlorophenyl derivatives the observed structural patterns resemble those found in crystals based on the tetra(4-hydroxyphenyl)porphyrin host, tentatively suggesting on the basis of this analogy that Cl···Cl attractions play a particularly important role in directing the interporphyrin organization of the chloro-substituted materials [6, 7].

The ability of a halogen group to steer crystal packing modes when substituted on an aromatic moiety, first proposed by Schmidt [8], is usually associated with the appearance of short halogen···halogen contacts. In molecular solids of chlorine and of bromine, for example, some observed nonbonding halogen···halogen contacts are significantly shorter than others and shorter than the sum of the corresponding van der Waals radii. Similar findings have been reported for a variety of organic structures [9, 10]. It is convenient to regard these short contacts as a manifestation of weak intermolecular bonding. The attractive and directionally anisotropic nature of these interactions has been also postulated on the basis of a recent survey of structural data in the Cambridge Crystallographic Database [11]. In this context, and in order to study additional crystal engineering aspects of microporous solids composed of tetraarylporphyrin building blocks, it was considered worthwhile to evaluate the structural features and the inclusion properties of the tetra(bromophenyl)metalloporphyrin system not studied before.

We report here the structure and crystal inclusion properties of zinc-tetra(4-bromophenyl)porphyrin [Zn—4BrTPP]. A comprehensive evaluation of the structural patterns in a series of newly prepared crystalline inclusion materials is presented below, including correlation of the observed features with those previously found for the chloro-substituted metalloporphyrin analogs. Thermochemical behaviour of selected systems is also reported. The solid porphyrin-based materials referred to in this investigation include:

1. Zn—4BrTPP [$C_{44}H_{24}Br_4N_4Zn$];

2. Zn—4BrTPP : pyridine [$C_{44}H_{24}Br_4N_4Zn \cdot C_5H_5N$] 1 : 3;
3. Zn—4BrTPP : mesitylene [$C_{44}H_{24}Br_4N_4Zn \cdot C_9H_{12}$] 1 : 4;
4. Zn—4BrTPP : aniline [$C_{44}H_{24}Br_4N_4Zn \cdot C_6H_7N$] 1 : 4;
5. Zn—4BrTPP : L-α-methylbenzylamine [$C_{44}H_{24}Br_4N_4Zn \cdot C_8H_{11}N$] 1 : 2;
6. Zn—4BrTPP : methyl salicylate [$C_{44}H_{24}Br_4N_4Zn \cdot C_8H_8O_3$] 1 : 2;
7. Zn—4BrTPP : benzylacetate [$C_{44}H_{24}Br_4N_4Zn \cdot C_9H_{10}O_2$] 1 : 1;
8. Zn—4BrTPP : ethylbenzoate [$C_{44}H_{24}Br_4N_4Zn \cdot C_9H_{10}O_2$] 1 : 2;
9. Zn—4BrTPP : bromobenzene [$C_{44}H_{24}Br_4N_4Zn \cdot C_6H_5Br$]1 : 1;
10. Zn—4BrTPP : *p*-xylene [$C_{44}H_{24}Br_4N_4Zn \cdot C_8H_{10}$] 1 : 1;
11. Zn—4BrTPP : dimethylsulphoxide [$C_{44}H_{24}Br_4N_4Zn \cdot C_2H_6OS$] 1 : 2.

2. Experimental

2.1. MATERIALS

The inclusion materials were obtained by recrystallization of the commercially available porphyrin host (MidCentury Chemicals, Posen, Illinois – standard literature methods for the preparation of the porphyrin compounds are given in Refs. [12] and [13]) from saturated solutions of the respective guest solvents. Crystals of pure Zn-4BrTPP were obtained from anisole.

2.2. STRUCTURE DETERMINATION

The crystallographically analysed single crystals were covered by an epoxy resin in order to avoid their deterioration during the diffraction experiments. Full details of the routinely applied experimental procedures are reported in previous publications of this series [5–7]. Diffraction data were collected at 298 K on an Enraf-Nonius CAD4 diffractometer using graphite monochromated MoK_α (λ = 0.7107 Å) radiation and the ω–2θ scan method. Crystal stabilities were checked by periodic monitoring of three reference reflections from different zones of the reciprocal space. Data were corrected by Lorentz and polarization factors, and empirical absorption corrections were applied. The structures were solved by direct methods using SHELXS-86 [14], and then refined by least-squares using the SHELXL-93 program [15]. As in related studies of analogous materials, the precision of the detailed crystallographic determination is reduced in some cases by the poor quality of the diffraction data resulting from low stability of the crystalline solids, as well as by structural disorder of the constituent species [5–7]. In the present case it is also decreased by the presence of four heavy bromine atoms in the host material. The refinement calculations were based on F^2. Non-hydrogen atoms of the porphyrin hosts were treated anisotropically, except in **3** where all the carbon atoms were isotropic. Atoms of the disordered guest components in **3**, **5**, **6** and partly in **7** were also refined as isotropic. The hydrogen atoms were introduced in calculated positions with isotropic U, the methyls being treated as rigid groups. The low number of 'observed' reflections and guest disorder often required application of

Table I. Summary of crystal data and experimental parameters for compounds **1–7**.

Compound	**1**	**2**	**3**	**4**	**5**	**6**	**7**
FW[a]	993.7	1231.0	1474.5	1366.2	1236.0	1298.0	1143.8
Space group	$P2_1/n$	$C2/c$	$P2_1$	$P\bar{1}$	$P1$	$P\bar{1}$	$P\bar{1}$
Z	2	4	2	1	1	1	2
a, Å	10.204(3)	25.037(9)	12.891(2)	9.822(2)	11.091(2)	9.040(5)	9.818(4)
b, Å	9.172(3)	9.586(3)	10.318(6)	10.559(3)	11.854(2)	12.287(8)	15.030(6)
c, Å	20.741(8)	24.537(6)	26.156(6)	15.218(9)	12.908(3)	13.010(9)	17.057(7)
α, deg	90.0	90.0	90.0	78.63(3)	116.13(2)	81.86(5)	111.24(4)
β, deg	103.3(2)	120.09(2)	90.40(2)	77.15(2)	110.72(2)	79.66(5)	102.27(3)
γ, deg	90.0	90.0	90.0	81.99(1)	98.14(2)	69.09(5)	98.37(3)
V,Å^3	1891.2	5095.4	3478.9	1501.0	1332.7	1323.3	2223.0
D_c, g cm^{-3}	1.74	1.60	1.41	1.51	1.54	1.62	1.71
$F(000)$	972	2448	1500	686	618	646	1132
μ, mm^{-1}	4.91	3.67	2.70	3.12	3.50	3.54	4.20
2θ limits, deg	50	50	48	50	50	50	46
N (unique) > 0	2893	3443	4463	2449	4236	4047	4880
L.S. parameters	217	299	318	273	498	246	494
$N\,[I > 2\sigma(I)]$	2018	1646	2439	1614	3032	2744	2504
$R_F\,[I > 2\sigma(I)]$	0.061	0.092	0.089	0.070	0.064	0.077	0.101
G.o.f. on F^2	1.06	0.95	0.87	1.17	0.60	1.05	1.00
$\lvert\Delta\rho\rvert_{max}$	1.10	0.50	0.54	0.54	0.45	0.76	1.13

[a]Formula weights refer to the compositions defined in the text.

geometric constraints (the phenyl groups were usually treated as rigid hexagons) and restraints in the refinement calculations in order to facilitate convergence and prevent unreasonable distortion of the molecular structure of the disordered fragments. Nevertheless, for structures **1** and **4–6**, and to a somewhat lesser extent for **2**, **3** and **7**, the refinements converged at reasonably low values, allowing a reliable description of the atomic parameters and of the intermolecular organization and interaction scheme. Although in structures **1** and **7** relatively high residual peaks ($\sim$1 e Å^{-3}) appeared in the vicinity of peripheral bromine substituents which exhibit large-amplitude thermal motion, the final difference-Fourier maps for these structures showed no indication of incorrectly placed or missing atoms. Crystals of the inclusion compounds **8–10** are not sufficiently stable under laboratory conditions and tend to deteriorate quickly. Thus, only the crystal data are available for these materials, but a comprehensive crystallographic analysis could not be performed. No further efforts were made to analyze these structures in detail, as they appear to be structurally isomorphous with other inclusion compounds, the intermolecular organization in which is already known. Compound **11** formed only powdered samples; the host–guest composition of this material was determined by thermal analysis.

The crystal data and pertinent details of the experimental conditions for compounds **1–7** are summarized in Table I. The crystal data for the other materials are: (**8**) triclinic, a = 8.88(1), b = 12.10(1), c = 13.71(4) Å, α = 79.6(2), β = 81.0(2) and γ = 69.5(1)°; (**9**) triclinic, a = 16.963(11), b = 17.000(8), c = 18.244(9) Å, α = 72.40(4), β = 67.86(6) and γ = 62.52(4)°; (**10**) triclinic, a = 16.962(2), b = 17.072(2), c = 18.203(4) Å, α = 72.98(1), β = 68.46(1) and γ = 62.39(1)°. Compound **8** is isomorphous with **6**, as has been confirmed by partial refinement of the former. The structures of **9** and **10** appear to be isomorphous with that of the 1 : 1 triclinic clathrate of zinc-tetra(4-chlorophenyl)porphyrin with nitrobenzene (a = 16.729, b = 16.785, c = 18.231 Å, α = 72.08, β = 66.44 and γ = 62.12°) [7].

Lists of fractional coordinates and thermal parameters of the nonhydrogen atoms, atomic coordinates of the hydrogen atoms, as well as of bond lengths and bond angles for structures **1–7**, along with the atom labeling schemes used, have been deposited as supplementary material.

2.3. THERMAL ANALYSIS

Thermogravimetry (TGA) and differential thermal analysis (DTA) were performed using TA Instruments module 910 and system controller 2100. Before analysis, crystals were removed from their mother liquor, blotted dry on filter paper, and crushed. Sample weight, in the different experiments varied from 3 mg to 9 mg. A constant stream of argon (flow rate 60 mL per minute) was passed over the samples. The temperature range was typically 303–613 K at a heating rate of 10 K min^{-1}.

3. Results

3.1. STRUCTURE OF THE FREE HOST **1**

Figure 1 depicts the molecular structure of host **1**. It is characterized by an essentially planar porphyrin core, with deviations of the individual atoms from the porphyrin plane not exceeding 0.05 Å. The dihedral angle between the mean planes of adjacent pyrrole rings is less than 1°. The zinc ion is located exactly in the center of the porphyrin framework at Zn—N distances within the normal range of 2.035(6)–2.040(6) Å. The four bromophenyl substituents are almost perpendicular to the porphyrin core, the dihedral angles between the mean planes of the peripheral rings and the central moiety ranging from 72.5(1) to 75.8(1)°. These stereochemical features are typical of many of the metallated tetraphenylporphyrin moieties. In the crystal lattice of $P2_1/n$ symmetry, the porphyrin molecules are located on inversion centers (Figure 1). Layers of parallel porphyrin units in the ab plane of the unit-cell centered at z = 0 interpenetrate into layers centered at $z = \frac{1}{2}$, and are related to the former by the crystallographic glide symmetry. This type of intermolecular aggregation, associated with planarity of the porphyrin core, is apparently stabilized by weak ligating interaction between the central zinc ion of one moiety and bromine substituents of two adjacent porphyrin species approach-

ing from opposite sides of the inversion center. The corresponding Zn···Br contact distances are 3.346(2) Å. The significant role of these interactions in preserving the high symmetry of the molecular structure is best appreciated by comparison of the analysed structure with those of the previously studied analogous materials. Thus, the intermolecular aggregation in the zinc-tetra(4-fluorophenyl)porphyrin, lacking specific interactions between the porphyrin units, is associated with a severe ruffling of the metalloporphyrin core in order to optimize the dispersive interactions [7]. The porphine nucleus is also nonplanar with distorted aromaticity in the solvate-free crystal structures of tetra(4-chlorophenyl)porphyrin [16] as well as of zinc-tetraphenylporphyrin [17], due to crystal packing requirements.

The available crystalline complexes and solvates of the Zn(II)-tetra (bromophenyl)porphyrin host reveal three characteristic modes of intermolecular organization, representing different patterns of porphyrin–porphyrin interaction.

3.2. Monoclinic packing modes in complexes of the porphyrin host with pyridine and with mesitylene

The structure of the pyridine adduct **2** is illustrated in Figure 2. This compound can be best described as a bis(pyridine) complex of the porphyrin host. The two pyridine molecules occupy the axial coordination sites of the zinc ion, coordinating to it through the lone electron pair of the nitrogen atom. The bis(pyridine)porphyrin entity is located on crystallographic centers of inversion. The porphyrin core is nearly planar, with the metal ion located in its center. The observed distances around the zinc ion in the six-coordinate structure are Zn—N(pyrrole) 2.049(11) and 2.053(13) Å, and Zn···N(pyridine) 2.483(16) Å. The latter metal-to-axial ligand distance is somewhat longer than in the related six-coordinate structures of low-spin Fe-tetraphenylporphyrin with pyridine ligands [18] and of the coordination polymer of Zn-tetrapyridylporphyrin [5]. The bis(pyridine)metalloporphyrin units are densely packed in layered zones extending parallel to the *(ab)* faces of the unit cell. The two layered arrangements centered at $z = 0$ and $z = \frac{1}{2}$ relate to each other by the screw symmetry (Figure 2), and resemble a 'herringbone' pattern [4]. Voids which form between adjacent sheets are occupied by an additional molecule of the solvate; this pyridine species is located in the crystal on the twofold axis of rotation at $0, y, \frac{1}{4}$.

A similar intermolecular organization of the 'herringbone'-type is observed in the crystal structure of **3**. This compound represents a 1 : 2 metalloporphyrin π-complex with mesitylene, in which molecules of the latter are arranged, at a relatively short distance, nearly parallel to the porphyrin core from above and below (Figure 3). The Zn ion is located in the plane of the porphinato ring. Along the axial directions the shortest Zn···C(mesitylene) contacts are 3.24(2) and 3.30(2) Å. The interplanar distances between the overlapping and interacting aromatic segments of the porphyrin and mesitylene constituents are within 3.3–3.5 Å. The π–π interaction between the porphyrin and the surrounding ligands is evidently hindered to some

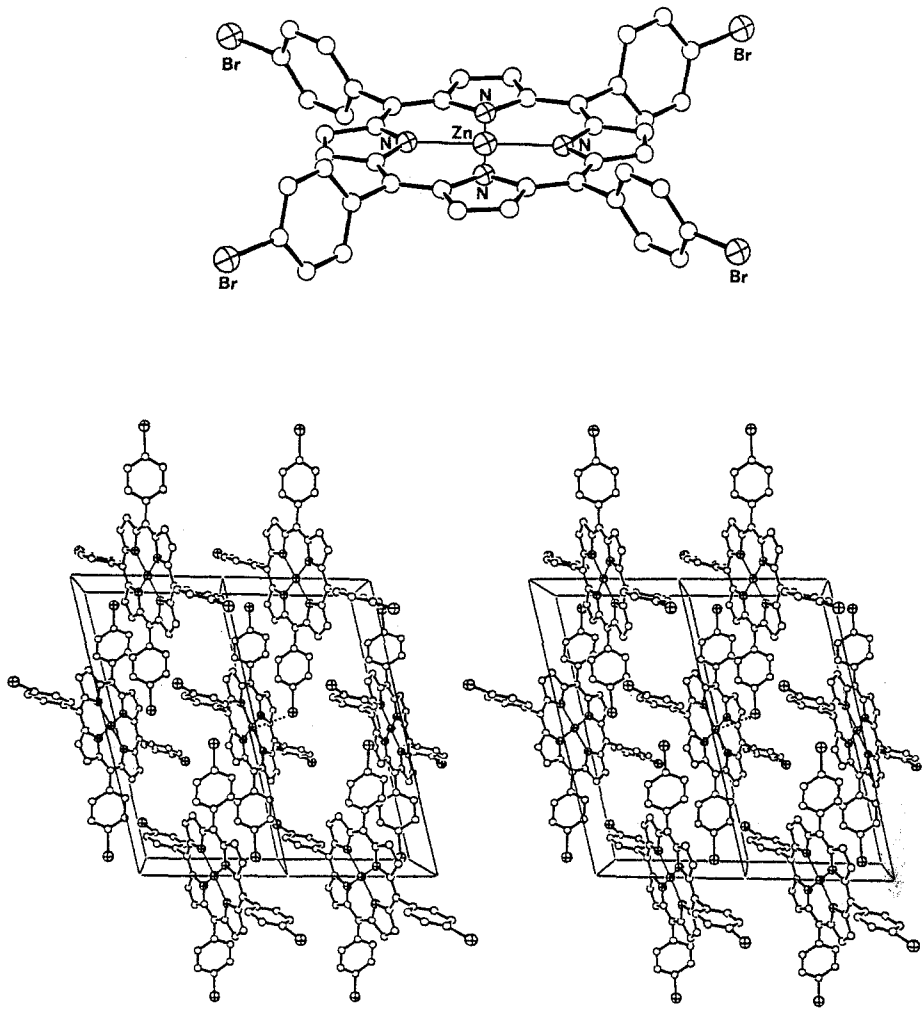

Figure 1. (Top) The molecular structure of zinc-tetra(4-bromophenyl)porphyrin. (Bottom) Stereoview of the crystal packing in **1** approximately down the **b**-axis (two unit cells are shown). The zinc ion is located on a crystallographic inversion center, and is approached from both sides by the Br-substituents of adjacent molecules at Zn···Br = 3.35 Å (one such contact is marked by a dotted line in the center of this figure).

extent by the bulkier methyl groups on the latter. The equatorial coordination of the metal ion is characterized by Zn···N distances within the range of 2.02(2)–2.05(2) Å. The porphyrin plane is slightly ruffled, several atoms deviating from planarity of the porphinato ring by 0.1–0.2 Å. The displacements are irregular, being most probably affected by the poor quality of the crystals and of the diffraction data in this case, and by a low data-to-parameters ratio in, and poor convergence of, the corresponding crystallographic refinement. As in the previous example, gaps

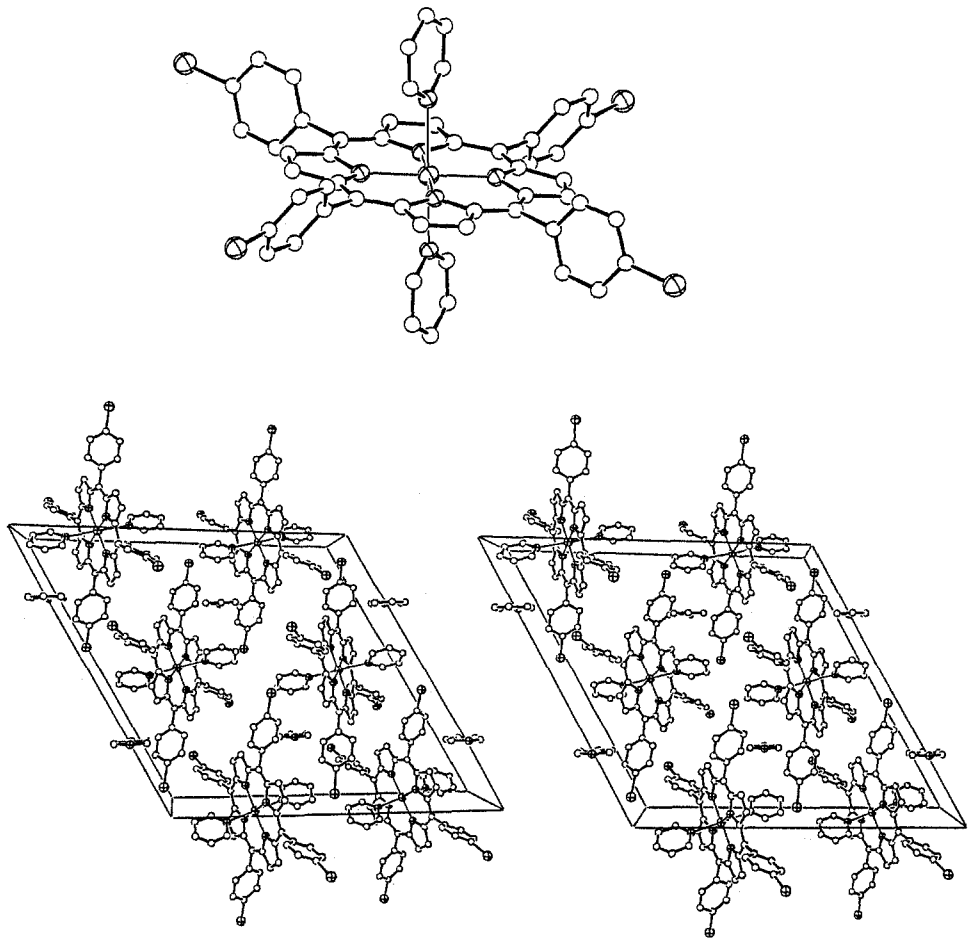

Figure 2. (Top) Molecular structure of the 1 : 2 complex of Zn—4BrTPP with pyridine. (Bottom) Stereoview of the crystal structure of **2** down the **b**-axis. Note that additional uncoordinated pyridine molecules are trapped in the crystal lattice between units of the complex.

between the bis(mesitylene)metalloporphyrin entities in the crystal structure are filled by two additional molecules of the mesitylene solvate.

3.3. INTERPORPHYRIN PATTERNS EXHIBITING C—BR···π(ARYL) INTERACTIONS

Compound **4** also represents a typical centrosymmetric six-coordinate complex of the metalloporphyrin entity. The zinc ion is located in the center of the nearly planar porphyrin core, and its axial coordination sites are occupied by two aniline ligands. The geometry of the zinc coordination is a distorted octahedron with equatorial Zn···N(pyrrole) and axial Zn···N(aniline) distances of 2.040–2.049(7) Å and 2.474(1) Å, respectively. The aniline ring is inclined with respect to the porphinato ring, the corresponding angle between the normals to the mean planes of these

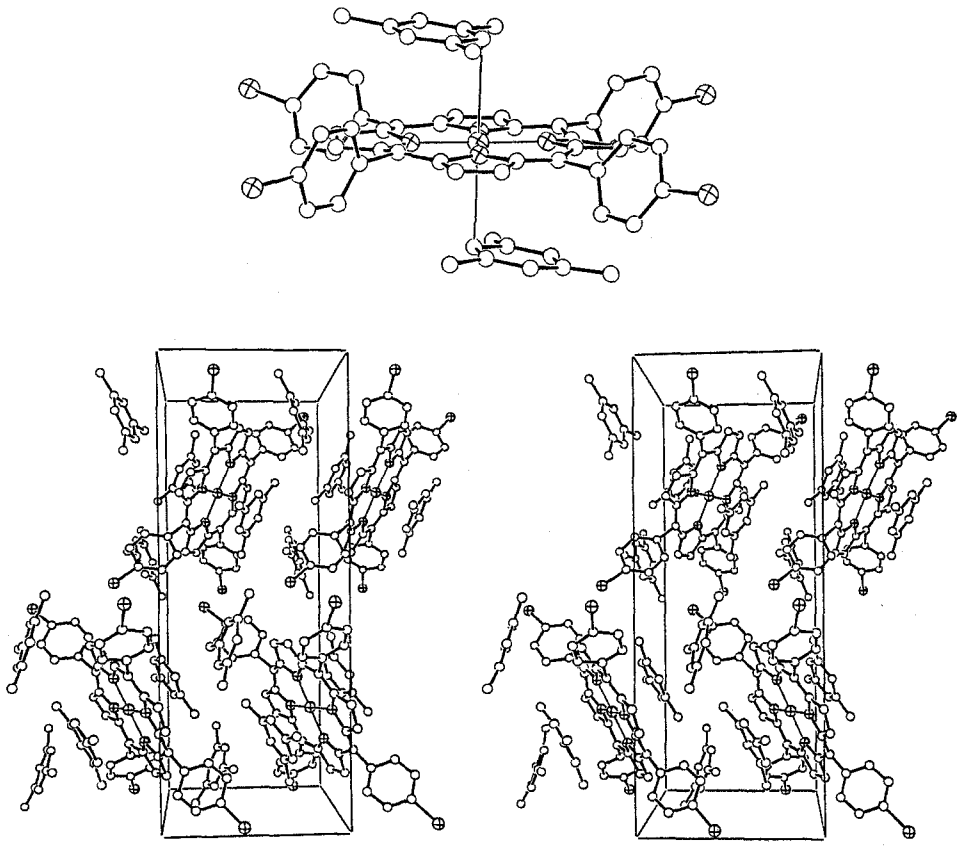

Figure 3. (Top) The 1 : 2 π-complex of Zn—4BrTPP with mesitylene. The shortest interatomic contacts between the zinc ion and the axial ligands, at Zn· · ·C(mesitylene) distances of 3.24(2) Å and 3.30(2) Å, are indicated. (Bottom) Stereoview of the crystal structure of **3** approximately down the **a**-axis. Mesitylene molecules coordinated to the porphyrin units as well as those entrapped between them are shown.

two rings being 28.9(1)°. A cross-section through the crystal parallel to the *ab* plane is depicted in the lower part of Figure 4. It illustrates the molecular structure of the bis(anilino)metalloporphyrin moiety, and the organization of these units in corrugated layers perpendicular to the plane of the projection. The upper part of Figure 4 shows the condensed translational relationship between adjacent porphyrin species displaced along the *c*-axis of the crystal, along with two additional aniline molecules which fill the interlayer voids. The latter species are not involved in any intermolecular coordination, and are partly disordered (they were modeled in the refinement calculations by geometrically constrained aniline frameworks with isotropic thermal parameters for the individual atoms). The T-shape arrangement between the bromophenyl arms of adjacent molecules is very similar to the typical interporphyrin organization in a large number of unsubstituted tetraphenylpor-

phyrin clathrates [4], as well as in many other compounds containing aryl groups [19, 20]. In this structure the C—Br bond of one species is nearly perpendicular to, and is pointing at, the bromophenyl ring of another species, the distance between the Br atom and that ring being 3.592(2) Å – slightly less than the sum of the corresponding van der Waals radii (3.65 Å). The close proximity between the Br atom of one porphyrin and the pyrrole C—H groups of the neighboring porphyrin located across an inversion center at 0, $\frac{1}{2}$, 1 [CH···Br = 4.03(1) Å] provides an additional hydrogen-bonding-type contribution to the stability of the tight interporphyrin organization in this direction. The shortest intermolecular Br···Br distance is only 4.137(2) Å, reflecting on a negligible contribution of direct halogen-halogen interactions to the stabilization energy of this structure.

The apparent —C—Br···π(bromophenyl) interaction which is associated with the T-shape organizational feature is even more pronounced in structure **5**. This compound is a chiral five-coordinate complex of the metalloporphyrin molecule with L-α-methyl-benzylamine. However, the well known tendency of the tetraphenylporphyrin moiety to form centrosymmetric arrangements in a condensed environment [1–4] in this case yields a pseudosymmetric disordered structure in which the concave surface of the five-coordinate complex is approached by a second guest molecule (Figure 5). It appears that these 1 : 2 metalloporphyrin-methylbenzylamine clusters are randonmly oriented in opposite directions at the different sites of the crystal lattice. The crystallographic refinement of the disordered structure in space group $P1$ assumed a possible disorder of the zinc ion (displacement above and below the porphyrin plane) with respect to the tetra(bromophenyl)porphyrin framework. An apparent rotational disorder of the —$CH(NH_2)CH_3$ tail in one of the methylbenzylamine molecules which is not anchored to the zinc had to be also accounted for by assigning partial occupancies to the amine and methyl residues. The refinement calculations indicated, by best convergence, that in the analysed crystal about 71(5)% of the clusters are oriented in one direction, while 29% of them are directed in the opposite direction. The main structural parameters of the molecular structure derived from the major orientation include deviation of the zinc ion by 0.335(7) Å from the plane of the four pyrrole nitrogens towards the axial ligand, and the Zn···NH_2(guest) coordination distance of 2.23(2) Å; the corresponding parameters for the minor orientation [0.57(1) Å and 2.25(6) Å] are less precise. In the resulting structural model the porphyrin moiety is severely distorted from planarity, but it is difficult to assess to what extent this represents a genuine structural feature of this species, or an artifact due to an incomplete description of the disordered model.

The interporphyrin organization exhibiting the 'T'-interactions in this structure is shown in Figure 5. The section shown involves two chains of densely packed porphyrins, and a row of guest molecules intercalated between them. The latter coordinate to metalloporphyrin species of neighboring layers approaching from above and below. The relevant intermolecular distances involving bromine between adjacent species in a layer are C—Br···π(aryl) = 3.384(3) and 3.446(3) Å

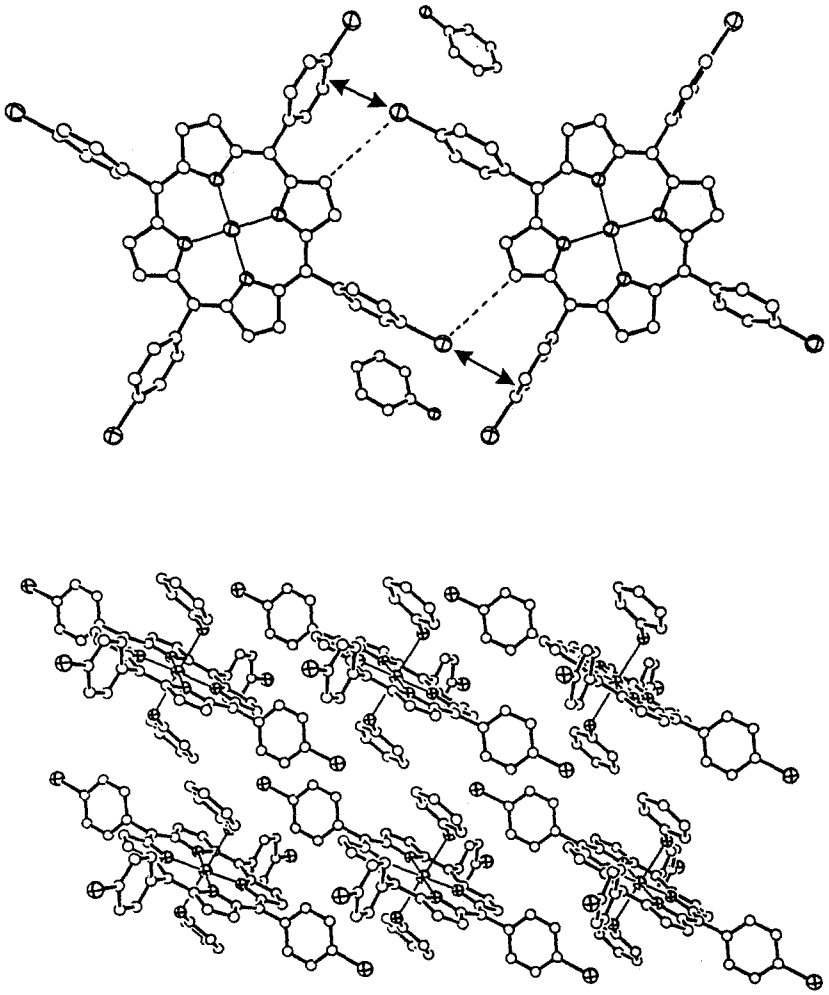

Figure 4. Illustration of the intermolecular arrangement in **4**. (Bottom) Close intermolecular packing of the 1 : 2 porphyrin complex with aniline in sheets parallel to the *ab*-plane of the crystal. (Top) The 'T'-shape arrangement of adjacent porphyrin units displaced along the **c**-axis. The dark arrows and the dashed lines mark C—Br···π and C—H···Br interactions, respectively. The two aniline molecules shown are not coordinated to the metalloporphyrin entities, filling voids between the porphyrin layers.

(displacement of the bromine atom from the corresponding plane of a neighboring phenyl ring which is perpendicular to the C—Br bond) and CH(pyrrole)···Br = 3.85(3) and 3.89(2) Å. Such distances are markedly shorter than the sums of the corresponding van der Waals radii, indicating a favourable contribution of these interactions to the stabilization energy of the observed pattern. The shortest intermolecular Br···Br contacts in this arrangement are $\geq$4.048(4) Å. The above

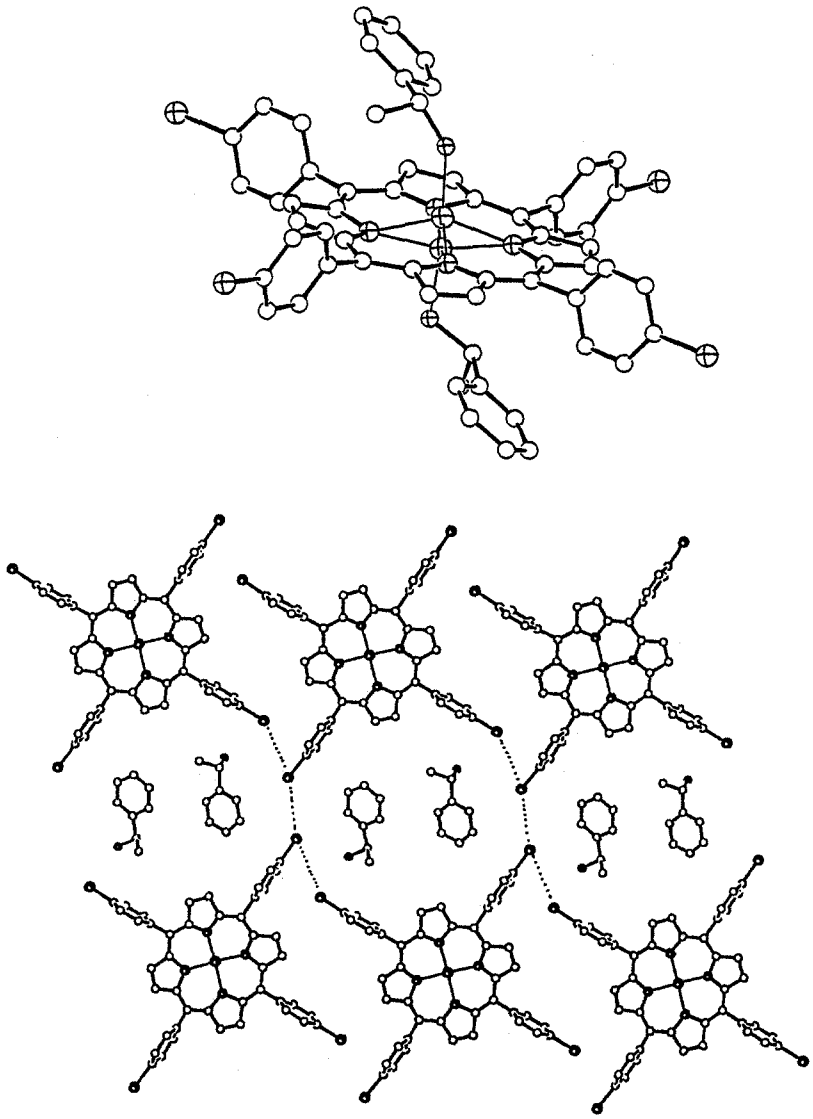

Figure 5. Structural features of **5**. (Top) A perspective view of the orientationally disordered porphyrin-methylbenzylamine adduct, showing its two possible orientations. Only one methylbenzylamine molecule is coordinated to the zinc ion at any given site in the crystal, the other filling the lattice space on the concave side of the five-coordinate complex. (Bottom) Two interporphyrin chain motifs characterized by 'T'-shaped interaction between molecules along the chain are shown. The dotted lines mark the shortest halogen···halogen approaches in this structure type. The ligands located between the chains coordinate to similar layers of porphyrin units located above and below.

described structural features of **5** are remarkably similar to those found in the analogous compound of the tetra(chlorophenyl)porphyrin derivative [7].

3.4. INTERPORPHYRIN ORGANIZATION IN POROUS LAYERS

The six-coordinate 1 : 2 porphyrin-methyl salicylate complex **(6)** and the 1 : 1 benzylacetate clathrate of the four-coordinate metalloporphyrin **(7)** reveal a characteristic mode of supramolecular interporphyrin organization, which has previously been observed in numerous structures of the tetra(hydroxyphenyl)porphyrin and tetra(chlorophenyl)porphyrin derivatives [6, 7]. The dominant structural motif in both structures consist of linear chains of nearly coplanar porphyrin species in which the Br-ends of the *cis*-related bromophenyl arms of one molecule face directly the peripheral Br sites of adjacent molecules in the chain (Figures 6 and 7). This open arrangement contains sizeable interporphyrin voids that can accommodate suitable guest molecules. The linear motifs assemble quite efficiently in two-dimensional layers, by fitting the convex sites (with C—Br terminal groups) of one chain into the concave surfaces (consisting of C—H bonds of the pyrrole rings) of adjacent chains. This is associated with the formation of relatively short CH···Br contacts (H-bonding type interactions) between the different chains, as well as of an anti-parallel alignment at close proximity of about 3.4 Å of the bromophenyl fragments. Isomorphous patterns have been observed in numerous complexes and clathrates formed with the Zn-tetra(chlorophenyl)porphyrin host [7].

The molecular structure of **6** is characterized by a perfectly planar porphyrin core with the zinc ion located in its center, and at 2.038(7) and 2.042(6) Å from the pyrrole N-atoms. The two bidentate methyl salicylate ligands weakly coordinate to the zinc at the axial sites. They can do so either through the hydroxyl group or through the carbonyl nucleophile, while occupying more or less the same lattice space above and below the porphyrin core. This is reflected in the crystal structure by a twofold orientational disorder of the ligand molecules. Refinement of the disordered model indicated almost equal occupancy factors for the two possible orientations, with a slight preference of coordination to the zinc ion through the hydroxyl group [53% occupancy, and a shorter Zn···OH distance of 2.71(2) Å versus a Zn···O=C contact of 2.94(3) Å at the second orientation]. Three-dimensional packing of the layered motifs is characterized by an effective fit of the axial ligands of one layer into the open interporphyrin voids of adjacent layers located above and below (Figure 6). The Br···Br contact between adjacent porphyrins along the circumference of these voids is 3.837(3) Å; the distance of these bromine atoms from the nearest pyrrole rings of neighboring molecules are CH···Br = 3.75(1) and 3.92(1) Å (the corresponding H···Br contacts being $\leq$3.0 Å).

Structure **7** is based on similarly layered four-coordinate metalloporphyrin units, with Br···Br contacts of 3.999(4) Å (Figure 7). Layers related by the inversion symmetry are stacked in an offset manner. The interporphyrin cavities formed between the two Br···Br edges in each layer are occupied by molecules of the

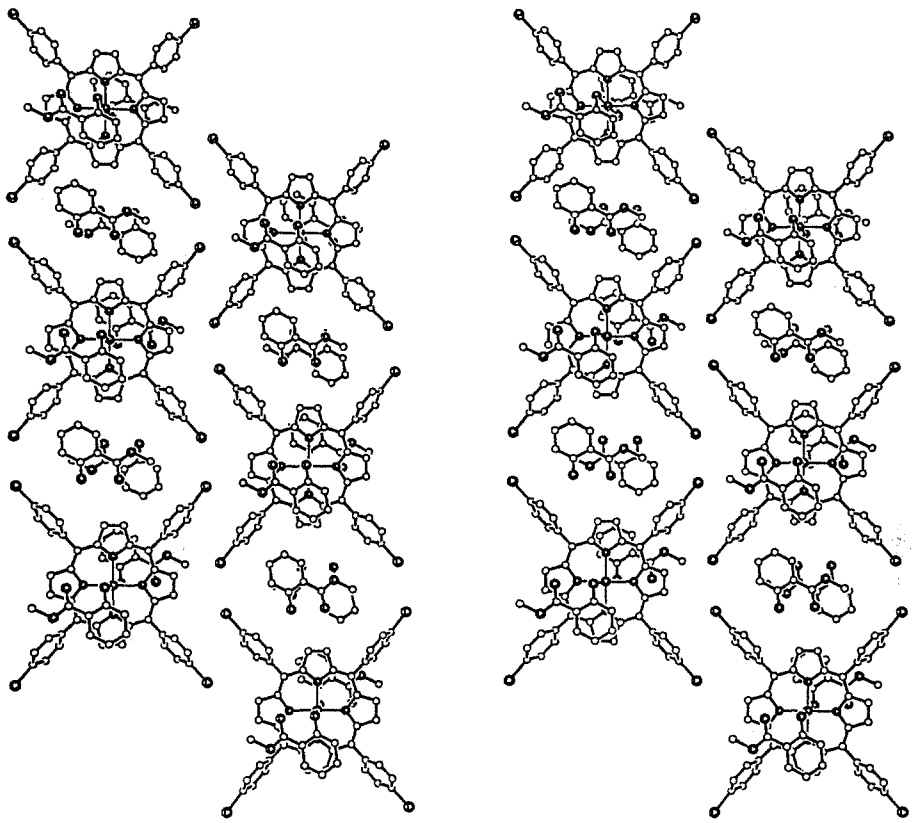

Figure 6. Stereoview of the intermolecular arrangement in **6** characterized by 'porous' layers of the porphyrin units, which stack one on top of the other in the crystal. The structure consists of 1 : 2 complexes of the title compound with methyl salicylate, the axial ligands of each layer being located in the interporphyrin pores of the upper and lower layers.

benzylacetate guest. The entrapped guests do not coordinate to the surrounding species, and exhibit large-amplitude thermal motion and/or partial structural disorder. Interporphyrin 'hydrogen-bonding' CH···Br distances in this structure range from 3.69(2) Å (H···Br = 2.9 Å) to 3.86(2) Å (H···Br = 3.0 Å). As is commonly observed for analogous four-coordinate porphyrin materials, the porphyrin core is severely distorted from planarity and adopts a 'saddle'-type conformation [7, 21]. Presumably, this allows minimization of the intermolecular steric hindrance and at the same time optimization of the dispersive interactions between the stacked layers. The tetrahedral distortion of the zinc coordination shell from ideal square-planar geometry has no marked effect (within the precision limits of this determination) on the Zn···N(pyrrole) distances, which vary from 2.011(11) to 2.025(11) Å.

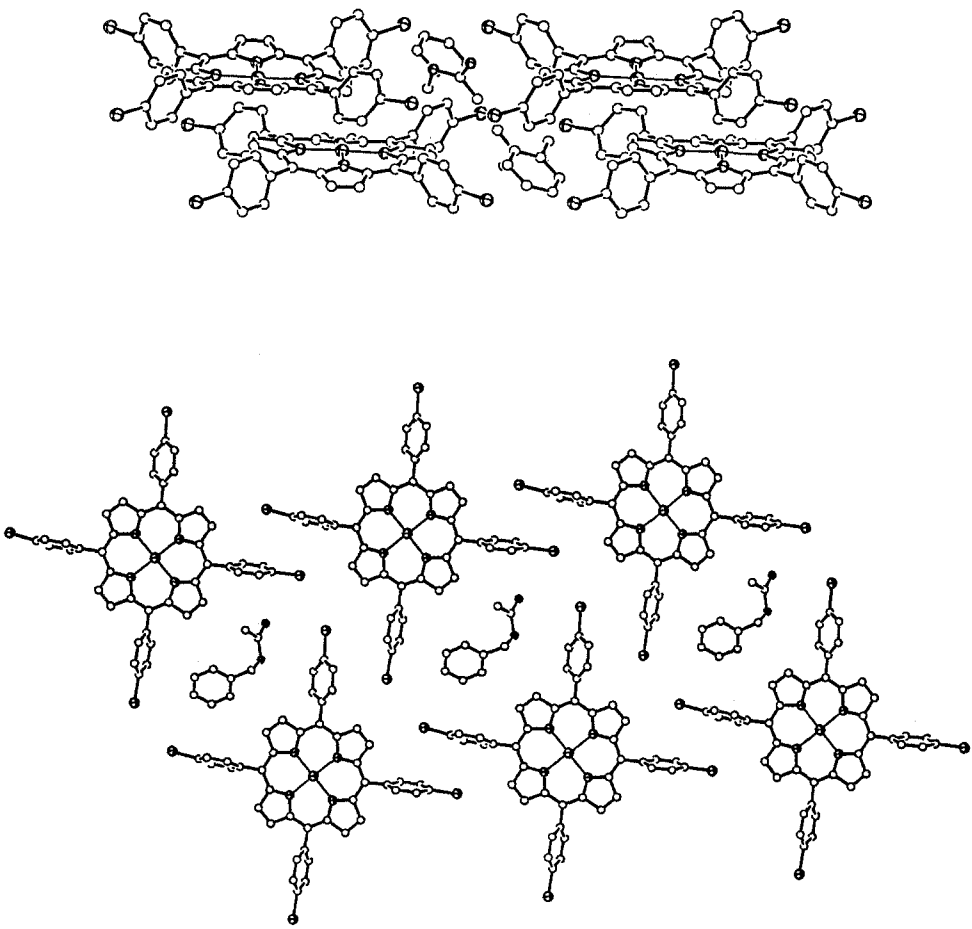

Figure 7. The crystal packing arrangement in **7**, illustrating enclosure of benzylacetate guest species within interporphyrin cavities of the 'O'-type structure. (Bottom) A single molecular sheet of nearly coplanar molecules. (Top) A side view showing the offset stacking mode of two adjacent layers.

3.5. THERMAL ANALYSIS

Gravimetric and differential thermal analyses were carried out on selected compounds in order to gain some insight into the guest release processes, to confirm the composition of those porphyrin clathrates which contain coordinated as well as uncoordinated guests, and to define the stoichiometry of compound **11** for which no single crystals could be obtained. The results of this study are summarized in Table II, and are also illustrated in Figure 8.

The TGA measurements clearly confirm the 1 : 3, 1 : 4 and 1 : 2 porphyrin–guest stoichiometries of compounds **2**, **4** and **6**. They also indicate that the stoichiometric

Table II. Summary of TGA-DTA data for compounds **2**, **4**, **6** and **11**.

Compound (host-guest ratio)	TG weight loss (%)		DTA guest release temp. (°C)	
	calculated	observed	onset	peak
2 (1 : 3)	19.25	18.19	130.8	140.9
			283.8	288.0
4 (1 : 4)	27.23	25.38	90.7	108.9
			145.5	156.9
6 (1 : 2)	23.42	21.21	91.2	102.5
11 (1 : 2)[a]	13.56	14.19	159.3	175.5

[a]Assumed to fit the observed weight loss, as the crystal structure could not be determined.

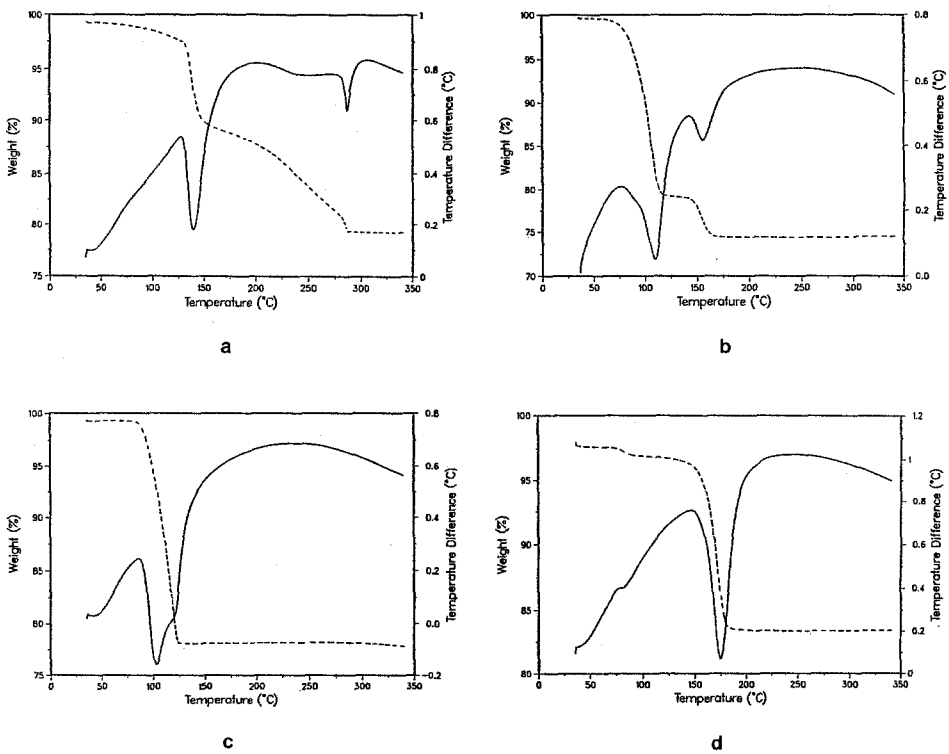

Figure 8. Thermal analysis data. TGA (dashed lines) and DTA (heavy lines) plots for the crystalline compounds (a) **2**, (b) **4**, (c) **6** and (d) **11**. Plots (a) and (b) represent a two-step decomposition process, while plots (c) and (d) indicate decomposition reactions mostly in a single step.

ratio in the porphyrin–DMSO complex **11** is approximately 1 : 2. A few qualitative conclusions can be drawn from the DTA results, which exhibit markedly different

characteristics for materials **2** and **4** than for **6** and **11**. In the former compounds the guest release process takes place in two steps, which is consistent with the presence of metal-coordinated as well as uncoordinated guest species in the crystalline lattice. Moreover, the pyridine adduct appears to be considerably more stable than that of aniline. Guest release from the six-coordinate complex **6**, containing a single type of guest component, appears to occur only in one step upon heating. The thermal behaviour of the DMSO adduct **11** also reveals a one-step decomposition. It further indicates that the interaction energy of the guest component with the metalloporphyrin is considerably stronger in **11** than in **6**.

4. Discussion

The relatively small number of the available crystalline adducts of zinc-tetra(bromophenyl)porphyrin, combined with the somewhat limited precision of the structural determinations in the present study, did not allow a rigorous evaluation of the corresponding molecular parameters. However, with respect to the metalloporphyrin host structure the available results conform well to previously reported experimental observations for differently substituted porphyrins [5–7], as well as to computational and experimental findings for unsubstituted tetraphenyl-metalloporphyrins [21, 22]. In all compounds the observed Zn···N(pyrrole) bonding distances are within 2.01–2.05 Å, the zinc ion fitting well into the center of the porphinato ring. The metalloporphyrin moiety deviates from planarity in five-coordinate as well as in four-coordinate materials due to coordination and crystal packing constraints. However, an almost perfect planarity of the metalloporphyrin core is usually preserved in the six-coordinate compounds in which both sides of the molecule are surrounded by a similar environment in the crystal lattice. The dihedral angles between the bromophenyl rings and the porphyrin ring vary in the different compounds between 67° and 107° in order to optimize the packing energy. Thus, ruffling of the porphyrin core and rotation of the substituent aryl groups within a limited range (more extensive rotation of the latter is sterically hindered by repulsion between the hydrogen atoms of the adjacent phenyl and pyrrole fragments) appear to be the softest modes of the molecular structure affected by intermolecular interaction in these compounds.

Divalent d^{10} zinc in inorganic compounds tends to achieve either four- or five-coordination [23]. However, in this series of studies on functionalized tetraphenyl-porphyrins we have observed not only four-coordinate and five-coordinate complexes, but also quite a significant number of six-coordinate metalloporphyrin entities (this report, and references [5–7]). The geometry of coordination varies from tetrahedrally distorted square-planar (ruffled four-coordinate compounds), through square-pyramidal (five-coordinate complexes), to tetragonally distorted octahedral (six-coordinate complexes) environments. As indicated by the structural data, there is a strong correlation between the binding strength of the axial ligands and the coordination number; the axial bond lengths being substantially longer in six-

Table III. Axial bond lengths of various ligands to the zinc-porphinato entity.

Ligating group	Bond length range (Å)	Reference
Five-coordinate compounds		
>S=O	2.12	[7]
pyridyl N:	2.13–2.15	[5]
—OH	2.19–2.21	[6,7], this work
aryl amine	2.20–2.23	[7], this work
—CH=O	2.22	[6]
—C(OR=O	2.28–2.40	[6]
Six-coordinate compounds		
pyridyl N:	2.36–2.39	[5]
pyridine N:	2.48	this work
aryl amine	2.47	this work
—OH (methanol)	2.46	[6]
—OH (aromatics)	2.68–2.71	[6,7] this work
—C(OR)C=O	2.68–2.70	[6,7]

coordinate than in five-coordinate structures. Evidently, frequent occurrence of the former is stabilized by crystal packing (including symmetry) requirements in the condensed solid phase. Furthermore, small and more basic ligands exhibit shorter bonds than larger and less basic ones. The relevant data are summarized in Table III, indicating that ligands containing the N: function (as well as the small DMSO and MeOH moieties) are bound to the zinc ion most effectively in the two modes of coordination. Axial coordination of aromatic ligands to and from both sides of the metalloporphyrin core through π–π interactions has also been observed in the various materials. The interacting ligands are usually aligned nearly parallel to the porphyrin plane at distances of about 3.4 Å.

Previous evaluations have shown that the crystalline architecture of tetraphenylporphyrin complexes and clathrates is dominated by the molecular shape of the large and nearly rigid porphyrin framework, yielding a very small number of interporphyrin arrangements [1–4]. It has also been shown that these packing modes can be modified to a considerable extent by functionalization of the tetraphenylporphyrin building blocks by various groups, including —Cl, at the *para* positions of the phenyl rings [5–7]. The bromosubstituted materials reported above exhibit various kinds of interporphyrin organization, differently affected by the halogen function. The pure host material **1** is unique among the tetraphenylporphyrins in the sense that it preserves an almost perfect planarity of the porphyrin core in the crystalline phase, due to apparent interaction of the metal center of one unit with the large and polarizable Br substituents of neighboring species. Compounds **2** and **3** form 'herringbone' type monoclinic arrangements, without any apparent

involvement of the halogen atoms in specific interactions. This mode of crystal packing is not very common among the tetraphenylporphyrin materials [4].

More typical is the interporphyrin organization observed in structures **4** and **5**, which resembles the 'T-type' packing motif found in a vast number of triclinic tetraphenylporphyrin clathrates [4]. It can be best described as consisting of continuous chains of metalloporphyrin molecules (or their complexes with axial ligands). These chains are characterized by a perpendicular arrangement of interacting bromophenyl groups and by a repeat distance of about 15.2 Å. They are stacked stepwise in corrugated sheets (Figure 4), intercalating solvent molecules between the sheets. The 'T'-shape interaction between bromophenyl groups on adjacent molecules of a chain is geometrically similar to that frequently found in solids of compounds which contain aromatic rings [19, 20], including in crystalline structures of the tetraphenylporphyrins [1–4], except that in this case C—Br$\cdots\pi$ interactions replace the C—H$\cdots\pi$ ones. The approach distances of the Br sites to the planes of neighboring aryl fragments (varying from 3.38 Å to 3.59 Å) are shorter than normal van der Waals contacts (3.65 Å), suggesting that these interactions provide a significant contribution to the stabilization energy of the observed interporphyrin arrangements (see below).

The expanded (labeled as 'O'-type) interporphyrin chain structure in compounds **6** and **7** is of particular interest, as it resembles the open hydrogen-bonded chain motif found in tetra(hydroxyphenyl)porphyrin materials [6]. Moreover, similar patterns occur quite frequently in the analogous tetrachlorophenyl derivatives of the metalloporphyrin, irrespective of the coordination number of the metal ion [6, 7]. The occurrence of halogen–halogen intermolecular close contacts, and their possible effect on preferred intermolecular organization in crystals of organic compounds, is also well documented in the literature [24, 25]. On the basis of these structural analogies it was initially tempting to assume that formation of the chain pattern is steered mainly by direct halogen–halogen interactions (instead of hydrogen bonding in the tetrahydroxyphenyl materials) between the Br-terminals of adjacent molecules which face one another along the chain (Figures 6, 7). Yet the relevant Br$\cdots$Br contacts of 3.84–4.00 Å observed in **6** and **7** are within a normal van der Waals range and do not provide convincing evidence for such a conclusion. A more detailed examination of the structural data suggested, in fact, that the stabilization of the observed architectures arises from a combination of different kinds of intermolecular forces, including those between adjacent chain motifs. The main features of these considerations are shown in Figure 9. It can clearly be seen that, in addition to the halogen-halogen contacts (marked by 'a' in this Figure), hydrogen-bonding type associations (marked by 'b') and dipolar interactions between bromophenyl groups aligned in an anti-parallel fashion (marked by 'c') contribute to the stability of the porous interporphyrin pattern.

It was of interest in the above context to assess the relative van der Waals stabilization energies of the 'T'-type and 'O'-type modes of interporphyrin organization. These were estimated by semiempirical computational methods using the

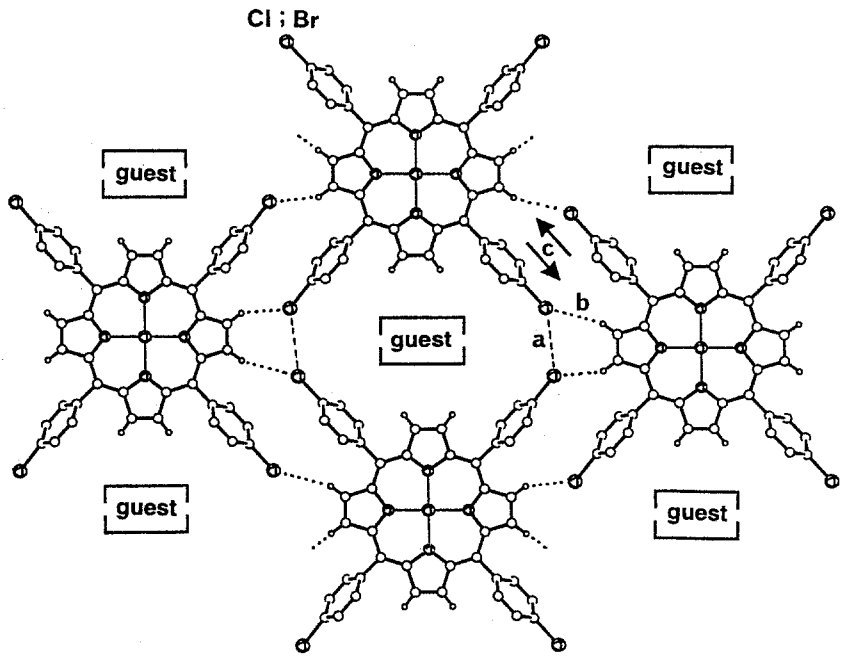

Figure 9. A detailed representation of the interporphyrin interaction pattern in structure **6** and **7**, most commonly observed also in crystalline assemblies of the zinc-tetra(4-chlorophenyl)-porphyrin building blocks. Dotted lines indicate (for X=Br or Cl) (**a**) X···X and (**b**) CH···X contacts ranging from 3.63 to 4.00 Å and from 2.7 to 3.1 Å, respectively. The dark arrows (**c**) mark dipolar attractions between partly overlapping bromophenyl or chlorophenyl groups of neighboring molecules aligned in an antiparallel fashion at a distance of about 3.4 Å.

Biosym software and standard atom-atom potentials [26], and the structural data obtained in our study. The results indicate that for the bromophenyl derivative the stabilization associated with O-type and T-type arrangements of two adjacent porphyrin molecules is of the order of −0.5 kcal/mol (in **4** and **5** – see Figures 4 and 5) and near −3.3 kcal/mol (in **6** and **7** – see Figures 6 and 7), respectively. When clusters of four molecules are considered, the intermolecular stabilization energy calculated for the layered 'O'-type pattern shown in Figure 9 is about −11.7 kcal/mol. For the 'T'-type structures, however, the highest stabilization energy of about −10.9 kcal/mol is associated with a four-molecule segment of a single porphyrin chain; the cohesive energy of two pairs of porphyrin molecules from adjacent chains involving Br···Br contacts is significantly lower (see Figure 5). On the basis of these data it appears that direct Br···Br interactions contribute negligibly to the stability of the 'O'-type pattern as well as to the 'T'-type structures, and that dipolar forces account for most of the intermolecular attraction. For a single chain of porphyrin molecules (and without accounting for additional interactions between the porphyrin and guest component), the 'T'-shape organization is clearly more favoured than the 'O'-shape pattern. However, when several chains in the

same layer are considered, there is no significant energy difference between the two structure types. Similar calculations, based on structural data reported in earlier publications [6, 7], were performed on two- and four-molecule arrays of the tetra(chlorophenyl)porphyrin units. For the latter compounds they showed quite a different trend. Thus, the pairwise porphyrin interaction energies in the 'T'-shape and 'O'-shape arrangements vary within 0–2 kcal/mol and 2–4 kcal/mol (in the repulsive range), respectively. When interactions between the chains are also considered involving four-molecule clusters, the calculated stabilization energies varied between −14 kcal/mol and −25 kcal/mol (net attraction) for the 'O'-pattern and between 0 and 6 kcal/mol (net repulsion) for the 'T'-pattern. Although these estimates are very crude and exclude possible charge-transfer contributions (which in fact were shown to be quite small for interactions involving halogen [25]), they provide a reasonable explanation of the experimental observations. Clearly, the halogen···halogen and C—halogen···π interactions are more attractive in compounds containing the more polarizable Br-group. The contribution of electrostatic dipolar forces to the stabilization energy is, however, considerably larger, and it is more significant in the chloro-substituted porphyrins than in the bromo-substituted ones due to the higher polarity of the C—Cl bond. Consequently, occurrence of the 'O'-type arrangement (Figure 9) is dominant among the tetrachlorophenyl derivatives [6, 7]. This is apparently not so for the inclusion compounds of Zn—4BrTPP, which in general appear to be less stable and more difficult to crystallize.

The available results of thermal analyses provide some qualitative indications on the relative thermodynamic stability of selected compounds and binding strength of the guest components within the porphyrin lattice. However, a more extensive effort is required in order to evaluate the dynamical and structural aspects of the phase transformations which are associated with the guest release process in the different materials.

Acknowledgement

This work was supported in part by the Israel Science Foundation administered by the Israel Academy of Sciences and Humanities, and by grant No. 94–00344 from the United States-Israel Binational Science Foundation (BSF), Jerusalem, Israel.

References

1. M.P. Byrn, C.J. Curtis, S.I. Khan, P.A. Sawin, R. Tsurumi, and C.E. Strouse: *J. Am. Chem. Soc.* **112**, 1865 (1990).
2. M.P. Byrn, C.J. Curtis, I. Goldberg, Y. Hsiou, S.I. Khan, P.A. Sawin, S.K. Tendick, and C.E. Strouse: *J. Am. Chem. Soc.* **113**, 6549 (1991).
3. M.P. Byrn, C.J. Curtis, I. Goldberg, T. Huang, Y. Hsiou, S.I. Khan, P.A. Sawin, S.K. Tendick, A. Terzis, and C.E. Strouse: *Mol. Cryst. Liq. Cryst.* **111**, 135 (1992).
4. M.P. Byrn, C.J. Curtis, Y. Hsiou, S.I. Khan, P.A. Sawin, K. Tendick, A. Terzis, and C.E. Strouse: *J. Am. Chem. Soc.* **115**, 9480 (1993).
5. H. Krupitsky, Z. Stein, I. Goldberg, and C.E. Strouse: *J. Incl. Phenom.* **18**, 177 (1994).
6. I. Goldberg, H. Krupitsky, Z. Stein, Y. Hsiou, and C.E. Strouse: *Supramol. Chem.* **4**, 203 (1995).

7. H. Krupitsky, Z. Stein, and I. Goldberg: *J. Incl. Phenom.* **20**, 211 (1995).
8. G.M.J. Schmidt: *Pure Appl. Chem.* **27**, 647 (1971).
9. G.R. Desiraju: in G.R. Desiraju (ed.), *Organic Solid State Chemistry*, Elsevier, Amsterdam, pp. 519–546 (1987).
10. G.R. Desiraju: in G.R. Desiraju (ed.), *Crystal Engineering – The Design of Organic Solids*, Elsevier, Amsterdam, pp. 175–201 (1989).
11. G.R. Desiraju and R. Parthasarathy: *J. Am. Chem. Soc.* **111**, 8725 (1989).
12. A.D. Adler, F.R. Longo, J.D. Finarelli, J. Goldmacher, J. Assour and L. Korsalioff: *J. Org. Chem.* **32**, 476 (1967).
13. J.S. Lindsey and R.W. Wagner: *J. Org. Chem.* **54**, 828 (1989).
14. G.M. Sheldrick: SHELXS-86. In G.M. Sheldrick, C. Kruger and R. Goddard (eds.), "Crystallographic Computing 3"; Oxford University Press 1985; pp. 175–189; *Acta Crystallog.* **A46**, 467 (1990).
15. G.M. Sheldrick: SHELXL-93. Program for the Refinement of Crystal Structures from Diffraction Data, University of Goettingen, Germany, 1993.
16. T. Hökelek, D. Ülkü, N. Günduz, M. Hayvali, and Z. Kiliç: *Acta Crystallogr.* **C49**, 1667, (1993).
17. W.R. Scheidt, J.U. Mondal, C.W. Eigenbrot, A. Adler, L.J. Radonovich, and J.L. Hoard: *Inorg. Chem.* **25**, 795 (1986).
18. N. Li, V. Petricek, P. Coppens, and J. Landrum: *Acta Crystallog.* **C41**, 902 (1985).
19. S.K. Burley and G.A. Petsko: *J. Am. Chem. Soc.* **108**, 7995 (1986).
20. G. Klebe and F. Diederich: *Phil. Trans. Roy. Soc. London A.* **345**, 37 (1993).
21. O.Q. Munro, J.C. Bradley, R.D. Hancock, H.M. Marques, F. Marsicano, and P.W. Wade: *J. Am. Chem. Soc.* **114**, 7218 (1992).
22. W.R. Scheidt and Y.J. Lee: *Struct. Bond. (Berlin)* **64**, 1 (1987).
23. F.A. Cotton and G. Wilkinson: *Advanced Inorganic Chemistry*, John Wiley & Sons, London, England (1980).
24. N. Ramasubbu, R. Parthasarathy, and P. Murray-Rust: *J. Am. Chem. Soc.* **108**, 4308 (1986).
25. S.L. Price, A.J. Stone, J. Lucas, R.S. Rowland, and A.E. Thorney: *J. Am. Chem. Soc.* **116**, 4910 (1994).
26. DISCOVER. Biosym Technologies, San Diego, California (1994).